Accelerated molecular dynamics of rare events using the local boost method

Jee-Ching Wang, Somnath Pal, and Kristen A. Fichthorn
Department of Chemical Engineering, The Pennsylvania State University, University Park, Pennsylvania 16802
(Received 27 June 2000; published 1 February 2001)

We present the *local boost method* for accelerating molecular-dynamics (MD) simulations of rare-event processes. To accelerate the dynamics, a bias potential is used to raise the potential energy in regions other than the transition states. This method reduces the number of MD time steps spent simulating motion in the potential-energy minima, and allows long-time simulations to be run. Correct equilibrium and dynamical quantities are achieved by using a time increment based on the principles of importance sampling. Two different bias potentials are probed. Both bias potentials are based on the potential energies of individual atoms. In both cases, the bias potential is turned on (off) when the energy of an individual atom is below (above) a boosting threshold energy. Implementing this method requires only minor modification to a conventional MD code, and the associated computational overhead is negligible. We demonstrate the method by applying it to the diffusion of atoms on Lennard-Jones fcc(001) and fcc(111) surfaces. Both single and multiple boosting-threshold energies are employed in these studies. These results show that the local boost method with multiple-boosting thresholds holds significant promise for application in large-scale MD simulations.

DOI: 10.1103/PhysRevB.63.085403 PACS number(s): 68.35.Fx, 02.70.Ns, 71.15.Pd, 82.20.Db

I. INTRODUCTION

A significant challenge in materials simulation is to conduct long-time simulations, while accurately retaining atomic-scale detail. A popular approach is molecular dynamics (MD), which provides accurate information on the details of atomic motion. However, MD simulations cannot currently proceed far beyond the nanosecond range. Thus long-time dynamics are inaccessible with this method. In systems where structural evolution occurs by a series of ''rare events,'' the dynamics can be characterized as a sequence of infrequent transitions from one potential-energy minimum to another. For such systems, the long-time dynamical behavior can be simulated as a series of jumps between potential-energy minima. The jump rate is given by transition-state theory (TST)[1–3] as the flux through a dividing surface that separates two potential-energy minima. If the TST rates are known accurately, then, in principle, a kinetic Monte Carlo (KMC)[4–7] simulation incorporating these rates can be used to reach macroscopic time scales, while retaining reasonable dynamical accuracy. However, for many systems it is difficult to ascertain the locations of all potential-energy minima and the TST hopping rates between them. This limits the accuracy of the KMC/TST approach.

To overcome the inadequacies of KMC and conventional MD approaches several recent studies[8–13] investigated the possibility of extending the time scale in MD simulations of systems with rare-event dynamics. The approach in these studies is to use importance sampling[14,15] to estimate dynamically the TST escape time for each minimum, as the system evolves via MD simulation. This is possible for systems with rare-event dynamics because the TST escape time is an equilibrium quantity associated with a particular minimum and a corresponding transition state. Efficient evaluation of the TST escape times can be achieved in this way, and the dynamics can be accelerated significantly by many orders of magnitude, depending on the potential-energy surface (PES) and temperature.

In one set of studies, Voter[8] showed that it is possible to accelerate rare-event dynamics by conducting MD simulations on a modified PES $V'(\{\mathbf{R}\})$ of the form $V'(\{\mathbf{R}\}) = V(\{\mathbf{R}\}) + \Delta V_b(\{\mathbf{R}\})$, where $V(\{\mathbf{R}\})$ is the original PES, $\Delta V_b(\{\mathbf{R}\})$ is the boost potential, and $\{\mathbf{R}\}$ denotes the full set of Cartesian coordinates for the N particles, $\{\mathbf{R}\} = \{\mathbf{R}_1, \ldots, \mathbf{R}_N\}$. The boost potential is designed to raise the potential energy near the minima with the constraint that the modified potential match the original one near all TST dividing surfaces. The energy barriers for escaping the minima on $V'(\{\mathbf{R}\})$ are smaller than on $V(\{\mathbf{R}\})$. Thus, fewer MD steps are required to escape from a minimum on $V'(\{\mathbf{R}\})$, and the simulation evolves faster than on the original PES. To map trajectories on $V'(\{\mathbf{R}\})$ onto $V(\{\mathbf{R}\})$, each time step receives a weighting factor to ensure that correct escape times are simulated for the original PES.[8] By constraining the potential to match the original one near the TST dividing surface, it is ensured that the probabilities of escape from a given potential-energy minimum satisfy detailed balance with various adjacent minima.

To construct a boost potential which yields correct equilibrium and time-dependent properties, it is necessary to ascertain dynamically when the system is in a minimum or at a transition state. In Voter's method[8] the boost potential depends on the smallest eigenvalue of the Hessian matrix $\mathcal{H}$ of second derivatives of the potential energy with respect to atomic positions. This eigenvalue becomes negative near a transition state and, thus, allows detection of transition states. However, manipulations of $\mathcal{H}$ add significant computational overhead to the simulation. Moreover, as the number of degrees of freedom increases, the probability that $\mathcal{H}$ will have negative eigenvalues away from the transition state increases and the method loses its efficiency.

In more recent studies, Voter improved on his original method. One of these studies focused on constructing the

boost potential without computing $\mathcal{H}$.[9] Here $\Delta V_b(\{\mathbf{R}\})$ is constructed from the two lowest eigenvalues of $\mathcal{H}$, which are found using only the gradient of the potential energy.[9] This method requires some advance knowledge of the PES in order to be effective. Another method (''parallel replica'') was also developed by Voter,[10] in which parallel computation is used to extend the time scale in the MD simulation of a small infrequent-event system. By integrating a replica of the system independently on each processor, observation of the first transition can be accelerated, and the method gives a correct transition-time distribution.

The approach of redefining the potential to obtain TST rate constants with MD has been used in previous studies.[11,16] To study structural transitions in macromolecular systems, Grubmüller[11] developed an elaborate MD scheme called ''conformational flooding.'' In this approach, conformational transitions in macromolecules are accelerated by the addition of a ''flooding'' potential into the Hamiltonian of the system, which in turn reduces the free-energy barrier heights. More recently, Steiner *et al.*[12] developed a simple boost potential in which the boosted potential energy is constant and equal to a fixed boost value if the potential energy falls below the boost value. In this method, Hessian manipulations are not performed. However, such a method is only effective for systems with a few degrees of freedom because fluctuations in the potential energy obfuscate transition states as the number of degrees of freedom increases. We recently introduced a simple boost potential which, with the proper choice of a boost parameter, guarantees that accurate TST escape times can be obtained with large acceleration to the dynamics.[13] In our method, similar to that of Steiner *et al.*,[12] the potential energy is boosted when it is lower than a fixed boosting threshold. We employed a smoothing function to ensure that the PES is continuous in the force from the boosted to the unboosted region. We showed that the smoothing function can also influence the boost in simulations of diffusion on a two-dimensional model PES.[13] In this paper, we extend and generalize our method to systems containing large numbers of atoms. In this method, which we denote as the *local boost method*, the boost is based on the potential energies of individual atoms. The method can be implemented with a single boosting threshold or with multiple boosting thresholds, to achieve greater efficiency in simulations of systems containing many different types of potential-energy minima. Below, we describe this method and demonstrate its application.

II. MODEL AND METHOD

We are interested in a system of N particles that resides in a multidimensional potential-energy well (state A) at a coordinate $\boldsymbol{\chi}(\{\mathbf{R}\},\{\mathbf{P}\})$, where $\{\mathbf{R}\}$ and $\{\mathbf{P}\}$ represent generalized coordinates and momenta, respectively. The rate constant $k_{TST}^{A\rightarrow}$ for escape from the potential-energy well (state A) is given by the canonical, ensemble-average flux exiting through the boundary to state A,[8]

$$k_{TST}^{A\rightarrow}=\frac{\int\int \dot{\boldsymbol{\chi}}\delta_A(\boldsymbol{\chi})\Theta_A(\boldsymbol{\chi})\exp[-\beta K(\{\mathbf{P}\})]\exp[-\beta V(\{\mathbf{R}\})]d\{\mathbf{R}\}d\{\mathbf{P}\}}{\int\int \exp[-\beta K(\{\mathbf{P}\})]\exp[-\beta V(\{\mathbf{R}\})]d\{\mathbf{P}\}d\{\mathbf{R}\}}, \tag{1}$$

where ''$\cdot$'' represents a time derivative, K is the kinetic energy, V is the potential energy, $\beta=1/k_BT$, $\delta_A(\boldsymbol{\chi})$ is a Dirac delta function applicable at the boundary to state A, and $\Theta_A(\boldsymbol{\chi})$ is unity when the system is in state A, and zero otherwise. In MD simulations, we naturally obtain the ensemble-average escape time, which is the reciprocal of Eq. 1, as the system evolves from minimum to minimum. However, prohibitively many time steps must be spent to access the transition states and, as a result, only limited dynamical evolution occurs.

In the local boost method (as in Voter's method[8]) the average escape time is accelerated through a bias potential $\Delta V_b(\{\mathbf{R}\})$, which is added to the original potential energy of the system $V(\{\mathbf{R}\})$. The biased PES $V'(\{\mathbf{R}\})$ has the form

$$V'(\{\mathbf{R}\})=V(\{\mathbf{R}\})+\Delta V_b(\{\mathbf{R}\}). \tag{2}$$

The bias potential ΔV_b is designed to increase the potential energy when the system is far from a transition state (thereby decreasing the number of MD steps necessary to reach the transition state), and to preserve the original potential in the vicinity of a transition state. This latter feature is necessary so that a detailed balance is maintained among different escape rates from various potential-energy minima. We investigated two possible forms for $\Delta V_b(\{\mathbf{R}\})$. In one of the versions investigated, $\Delta V_b(\{\mathbf{R}\})$ has the form

$$\Delta V_b(\{\mathbf{R}\})=V_{max}(\{\mathbf{R}\})\left(\frac{1-S(\{\mathbf{R}\})}{S(\{\mathbf{R}\})}\right), \tag{3}$$

where $V_{max}(\{\mathbf{R}\})$ is the maximum potential energy of all *individual particles*, i.e.,

$$V_{max}(\{\mathbf{R}\})=\max[V_i(\{\mathbf{R}\})], \quad i=1,\ldots,N, \tag{4}$$

where i denotes a specific particle, and N is the number of particles in the system. The function $S(\{\mathbf{R}\})$ ensures that the bias potential turns smoothly on (off) when the system is far from (near to) a transition state. To gauge the proximity of the system to a transition state, we also rely on the values of single-particle energies: if V_{max} is below a preset boosting

threshold V_b, then $S(\{\mathbf{R}\})>1$, and the potential energy is boosted[17]; if V_{max} lies above V_b, then $S(\{\mathbf{R}\})=1$ and $V'(\{\mathbf{R}\})=V(\{\mathbf{R}\})$. To uphold the detailed-balance criterion, V_b should be lower than the maximum single-particle energy when the system is at its lowest-energy transition state. Defining $\Delta V(\{\mathbf{R}\})=V_b-V_{max}(\{\mathbf{R}\})$, $S(\{\mathbf{R}\})$ has the form

$$S(\{\mathbf{R}\})=1+\Theta(\Delta V)f(\Delta V). \tag{5}$$

Here $\Theta(x)$ is a standard step function, such that $\Theta=1$ when $x\geqslant 0$, and $\Theta=0$ otherwise. The step function turns the boost on (off) below (above) the boosting threshold. The function $f(\Delta V)$ is included to ensure a smooth variation in the potential energy and continuity in the forces from the boosted to the unboosted regions of the PES. This function has the form

$$f(\Delta V)=\frac{c\exp(-\gamma/\Delta V)}{1+\exp(-\gamma/\Delta V)}, \tag{6}$$

where c and γ are tunable parameters that should not significantly influence the dynamics.[13]

A second form that we investigated for $\Delta V_b(\{\mathbf{R}\})$ is given by

$$\Delta V_b(\{\mathbf{R}\})=\Delta V_{min}(\{\mathbf{R}\})g(\Delta V_{min}), \tag{7}$$

where $\Delta V_{min}(\{\mathbf{R}\})$ is the minimum-energy difference between a single-particle potential energy and a boosting-threshold energy. For a single boosting-threshold energy, ΔV_{min} is equal to ΔV, as defined for Eq. (5). As we will demonstrate below, Eq. (7) can also be adapted for multiple boosting-threshold energies to increase the efficiency in large-scale simulations of systems containing many different types of minima. The function $g(\Delta V_{min})$ has the form

$$g(\Delta V_{min})=\Theta(\Delta V_{min})\left(\frac{c(\Delta V_{min})^n}{1+c(\Delta V_{min})^n}\right), \tag{8}$$

where Θ is a standard step function, as described above, and c and n are parameters.

For both forms of the bias potential presented above, the instantaneous force acting on a particle i residing on the boosted PES $V'(\{\mathbf{R}\})$ can be calculated from Eq. (2) for the desired form of ΔV_b. This requires the addition of a few lines to a conventional MD code, and the resulting computational overhead is negligible. It should be noted that since the local boost method is *local*, the forces will only be modified for the ''boosted'' particle [i.e., the particle with V_{max} in Eq. (3) or ΔV_{min} in Eq. (7)], and for particles within the potential cutoff of the ''boosted'' particle.

To illustrate the bias potentials employed here, we calculated the boosted PES for a one-dimensional potential $V(x)=-2.0-\cos(\pi x)$. In Fig. 1, we show the modified PES for the bias potential given by Eq. (3) with the smoothing function of Eq. (6). Although all potential energies below V_b are altered to some extent, the parameters c and γ control the properties of the boost. Figure 1(a) shows the influence of γ on the boosted PES. When γ is large (i.e., $\gamma=1$ and 2), the boost is conservative, and the shape of the boosted PES is similar to the shape of the original one. For aggressive boosting, such as with $\gamma=0.1$, subwells are created near $V(x)=V_b$. Another way to control the boost is to vary c. Figure 1(b) shows that larger values of c give larger boosts. As for γ, more aggressive boosting (larger c) creates additional subwells in the PES. From Fig. 1(c), we see that for fixed γ and c, the shapes of the boosted PES's are similar, and that V_b controls the amount of boost. Although it is not apparent

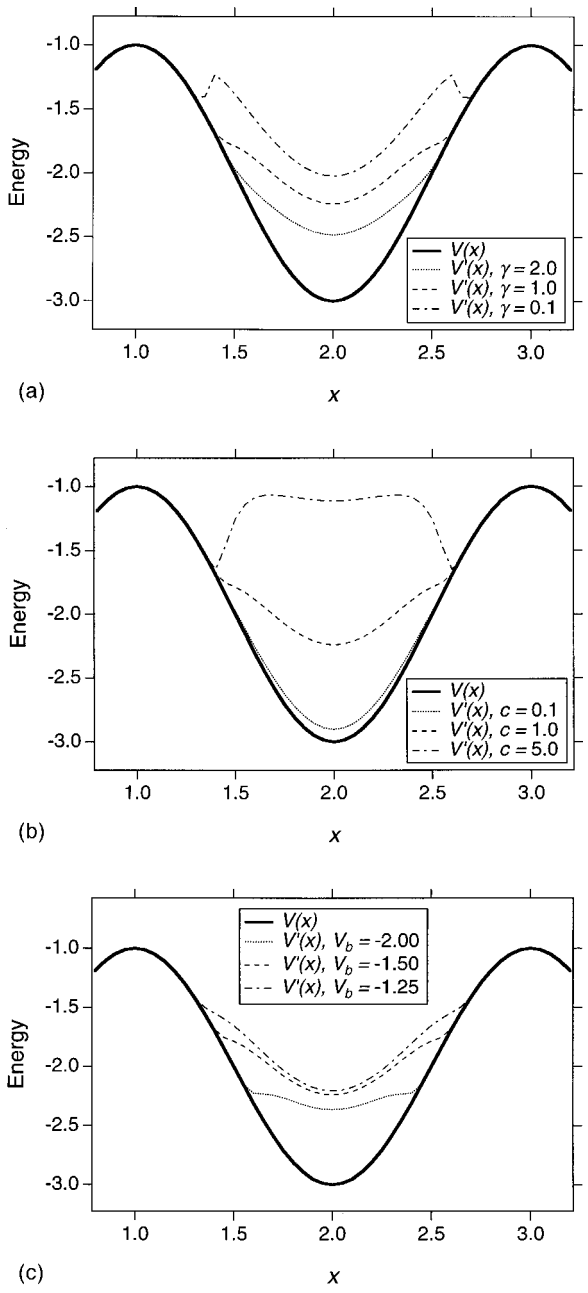

FIG. 1. Biased potentials $V'(x)$ for the potential $V(x)=-2.0-\cos(\pi x)$. The biased potentials are obtained using Eq. (3). We show the influence of (a) γ for $c=1.0$ and $V_b=-1.5$, (b) c for $\gamma=1.0$ and $V_b=-1.5$, and (c) V_b for $\gamma=1.0$ and $c=1.0$ on the boosted PES. The original PES is shown bold in each figure.

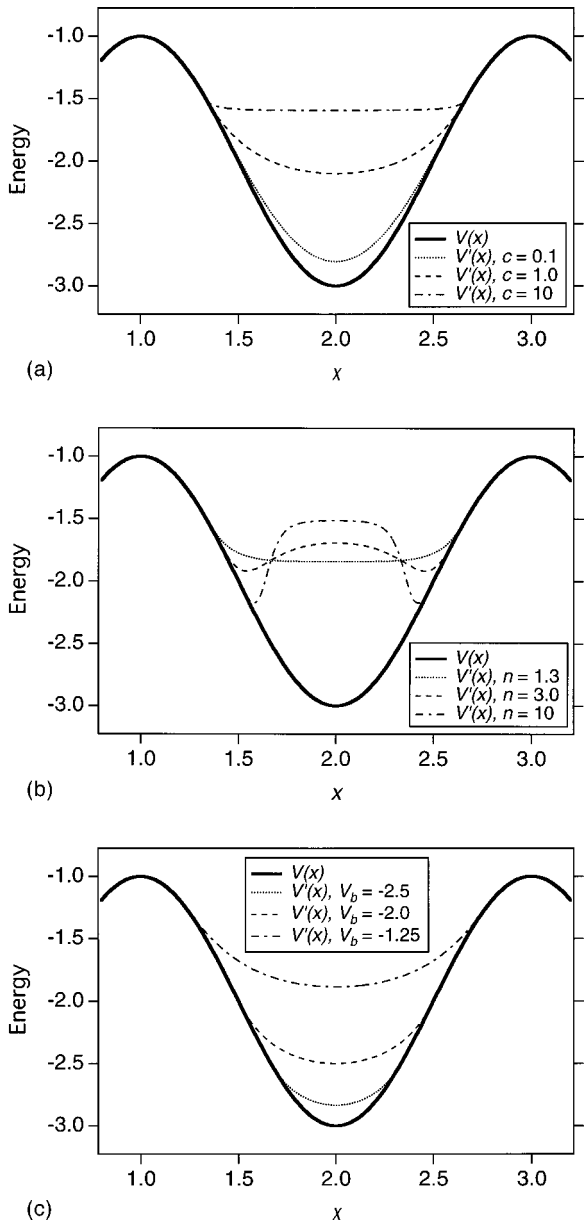

FIG. 2. Biased potentials $V'(x)$ for the potential $V(x)=-2.0-\cos(\pi x)$. The biased potentials are obtained using Eq. (7). We show the influence of (a) c for $n=1.0$ and $V_b=-1.5$, (b) n for $c=2.0$ and $V_b=-1.5$, and (c) V_b for $n=1.0$ and $c=1.0$ on the boosted PES. The original PES is shown bold in each figure.

from the figures, all the boosted PES's are continuous in the force as $\Delta V(x)\rightarrow 0^+$.

All of the PES's shown in Fig. 1 satisfy the criterion[8] that the boosted potential must be the same as the original near the transition-state region. Although this is an important criterion to be satisfied in achieving detailed balance, there are more subtle issues in choosing an appropriate boosting potential. In dynamical simulations, for example, the value of the ensemble-average escape time can be reduced by transition-state recrossing. It is known[20,21] that the extent to which this phenomenon occurs depends on the shape of the PES. The general guideline for choosing a biased PES is not yet well determined. However, for at least the one reason discussed above, we feel that surface shapes that are not drastically different than the original PES are good choices. For example, the biased PES with $c=1.0$, $\gamma=2.0$, and $V_b=-1.5$ [Fig. 1(a)] retains the shape of the original PES, and is most likely acceptable. However, the potential with $c=5.0$, $\gamma=1.0$, and $V_b=-1.5$ [Fig. 1(b)] should probably be avoided, unless its effects are carefully determined for a particular application. Actually, in our previous study,[13] we found that accurate results can be obtained from a PES with artificial subwells. One factor governing the accuracy in this case is the stiffness of the modified PES. The stiffness reflects the magnitude of the gradients on the PES, with larger gradients producing a more stiff PES. The function $S(\{\mathbf{R}\})$ [cf. Eq. (5)] determines the stiffness of the PES when a particle enters the region where its energy is less than the boosting threshold energy. In most applications, it is safe to have a relatively soft biased PES compared to the original PES, since this can prevent numerical instability, reduce the influence of subwells, and limit a quick exit of a particle to an adjacent state by reflection from the biased PES.

One drawback when the smoothing function given by Eq. (6) is used in Eq. (3) is that the PES loses its original shape and develops subwells when the potential energy is increased significantly above its original value. To remedy this problem, we consider a second form for $\Delta V_b(\{\mathbf{R}\})$, given by Eq. (7). It can be easily shown that when $n\leqslant 1$, c can take on any positive value without generating artificial subwells in the biased PES. Under these conditions, the biased PES becomes flatter as c increases, as shown in Fig. 2(a). For $n>1$, subwells can still be avoided with $c\leqslant[(n-1)\Delta V_{min}^{n}]^{-1}$, as shown in Fig. 2(b). The influence of V_b for fixed c and n is shown in Fig. 2(c). It can be seen that changing this parameter in Eq. (7) has a similar effect on the PES as it does for the bias potential given by Eq. (3) [cf., Fig. 1(c)].

In addition to having a well-defined parameter space in which subwells can be avoided, the bias potential given by Eq. (7) has the beneficial property that it is a function of energy differences. This feature can be contrasted to Eq. (3), which deals with specific particle energies. By incorporating energy differences, the boosting function in Eq. (7) becomes virtually independent of the minimum it is boosting. This is because the PES is generally expected to be harmonic near a minimum. Thus the parameters associated with this boosting function (i.e., the parameters whose effect we demonstrated in Fig. 2) should be transferrable to a wide variety of systems. In contrast, one generally needs to apply different values of the boosting parameters in Eq. (6) for different minima when using the bias potential given by Eq. (3). Because of its relative ease of transferability among various potential-energy minima, the bias potential given by Eq. (7) is more easily adapted to include multiple-boosting thresholds, as we will demonstrate below.

When accelerated MD simulations are run on a modified PES V', it is important to ensure that equilibrium averages of static and dynamical quantities on V' map directly to those on V. Using importance sampling techniques,[14,15] the TST rate constant in Eq. (1) can be expressed as

$$k_{TST}^{A\rightarrow}=\frac{\int\int \dot{\chi}\delta_A(\chi)\Theta_A(\chi)w(\beta,\{\mathbf{R}\})\exp[-\beta K(\{\mathbf{P}\})]\exp[-\beta V'(\{\mathbf{R}\})]d\{\mathbf{R}\}d\{\mathbf{P}\}}{\int\int w(\beta,\{\mathbf{R}\})\exp[-\beta K(\{\mathbf{P}\})]\exp[-\beta V'(\{\mathbf{R}\})]d\{\mathbf{P}\}d\{\mathbf{R}\}}, \tag{9}$$

where the weighting function $w(\beta,\{\mathbf{R}\})$ is given by

$$w(\beta,\{\mathbf{R}\})=\exp(\beta(V'-V)). \tag{10}$$

The weighting function is defined so that the averages given by Eqs. (1) and (9) are equal. This function determines how much weight is assigned to each configuration that can be reached by boosting to $V'(\{\mathbf{R}\})$, so that the weighted averages correspond to time averages on $V(\{\mathbf{R}\})$. Using Eq. (2), this weight can also be written as

$$w(\beta,\{\mathbf{R}\})=\exp(\beta\Delta V_b), \tag{11}$$

where $\Delta V_b(\{\mathbf{R}\})$ is given by Eqs. (3) and (7) for the two different forms probed here. To obtain correct time and ensemble averages, the boosted time increment $\Delta t'(\{\mathbf{R}\})$ is given by

$$\Delta t'(\{\mathbf{R}\})=w(\beta,\{\mathbf{R}\})\Delta t, \tag{12}$$

where Δt is the MD simulation time step. As in Voter's method,[8] time evolves in a coarse-grained manner and becomes a statistical property. Therefore, correct thermodynamic-average escape times are obtained only in the limit of long times.

At this point, it is important to stress certain aspects of the local boost method. In particular, the use of single-particle energies is central to this method. These energies are easily defined in semiempirical potentials, such as Lennard-Jones, embedded-atom method,[18] Stillinger-Weber,[19] etc., which are currently suitable for large-scale MD simulations. Implementation of the local boost method in *ab initio* MD simulations would require one to define individual atom energies in these simulations, which is not typically done. Our approach can be contrasted to a *global* approach involving the total potential energy. For such a boosting scheme, the method would only be efficient for systems with a few degrees of freedom. This is because fluctuations in the total potential energy obfuscate transition states. In an approach based on the potential energies of individual atoms, the proximity of each atom to a transition state is estimated, eliminating the fluctuation problem in a global approach. The construction of the potential-energy bias functions in Eqs. (3) and (7) ensures that the potential energy is boosted locally, where a transition is likely to occur. Because we alter the potential energy locally, it is unlikely that the system will be perturbed significantly by the bias potential. Thus the accelerated dynamical behavior of the system should faithfully represent what could be achieved in an *unaccelerated* MD simulation, if such a simulation could be run to long enough times.

A second aspect of the local boost method is that one is required to select appropriate boosting-threshold energies. By implementing this criterion for detecting the proximity of the system to a transition state, we avoid the computational overhead associated with diagonalizing the Hessian matrix that is implicit in Voter's method.[8] However, one has to choose boosting-threshold energies that are (i) sufficiently above the values of single-particle energies when the system is at a minimum (so that the dynamics are accelerated); and (ii) below the single-particle energies when the system is at a transition state (so that the detailed-balance criterion is upheld). If the minimum-energy configurations of a system can be ascertained (this is often the case, for example, in crystal growth), then it is possible, based on a knowledge of the energies of the minima, to choose boosting-threshold energies that can be refined during trial simulation runs prior to a production run.

To demonstrate various aspects of the local boost method, we applied it to the diffusion of Lennard-Jones (6-12) atoms on Lennard-Jones fcc(001) and fcc(111) surfaces. The Lennard-Jones potential employed here is truncated and shifted to zero at a distance of 2.5σ, where σ is the length parameter. We use the value of the bulk lattice constant for a Lennard-Jones solid, which is given by $a_0\approx 1.54\sigma$.[22] To model the fcc(100) and fcc(111) substrates, we use slabs that are seven atomic layers thick in the z direction [perpendicular to the (001) or (111) surface normal], with 50 [fcc(001)] or 70 [fcc(111)] atoms per layer to satisfy the minimum-image convention. We apply periodic boundary conditions in the x and y directions. The bottom three layers are fixed to their equilibrium crystal-lattice positions, and the fourth layer is used as a heat bath. To integrate the equations of motion, we used the velocity Verlet[23] algorithm for the top three layers and the Gaussian thermostat method[23,24] together with a scheme proposed by Brown and Clarke[25] for the heat-bath layer. The dimensionless time step $\Delta t^{\star}=0.0023129=\Delta t/(\sigma^2 m/\epsilon)^{1/2}$, where σ and ϵ are the length and energy parameters for the Lennard-Jones potential, and m is the mass of the atoms. For example, if we choose to model platinum, $\sigma=2.543$ Å, $\epsilon=0.679$ eV;[22] and $\Delta t\approx 1$ fs. The simulation system is rigorously equilibrated before each production run by continuously checking the average temperature, the temperature fluctuation, and the velocity distribution.

The tracer-diffusion coefficient D of the adatom is calculated in two different ways. In the first of these, we used the Einstein equation, in which D is given by

$$D=\lim_{t\rightarrow\infty}\frac{\langle\Delta\mathbf{R}^2\rangle}{2dt}, \tag{13}$$

where $\Delta\mathbf{R}^2=[\mathbf{R}(t)-\mathbf{R}(0)]^2$, $\langle\cdots\rangle$ denotes an ensemble average, and $d=2$ is the dimensionality of the surface. The

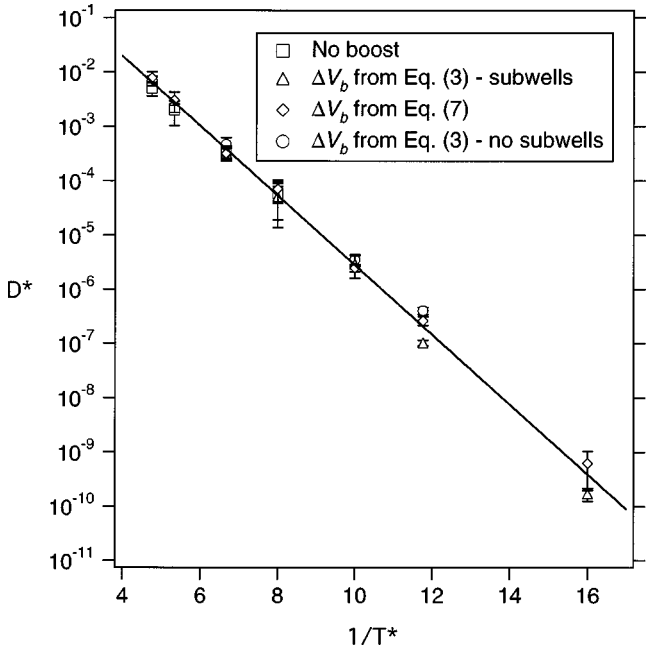

FIG. 3. Arrhenius plot of dimensionless tracer-diffusion coefficients $D^\star$ (as defined in the text) obtained via Eqs. (13) and (14) vs dimensionless reciprocal temperature $T^\star$ (as defined in the text). Results are shown for unbiased MD simulations (squares) and biased MD simulations using Eq. (3) (triangles and circles) and Eq. (7) (diamonds). The solid line is a fit through all data points obtained for biased PES with both Eqs. (3) and (7).

average value of D is estimated by converting the trajectories into $\Delta\mathbf{R}^2(t)$ vs t curves, and averaging over their slopes. This procedure is adequate for the higher temperatures, where the mobility is the largest and good statistics could be accumulated. However, for the lower temperatures, the adatom spends long time periods vibrating in the potential-energy minima, and its random walk between various binding sites may not always reach the diffusive regime. For the lower temperatures, we exploit the fact that surface diffusion is a rare-event process, in which D is given by

$$D=\frac{\lambda^2 n k_{TST}}{2d}, \tag{14}$$

where λ is the hopping distance which is the distance between nearest-neighbor minima in the systems studied here, n is the number of nearest-neighbor minima, and k_{TST} is the TST escape rate, given by Eq. (1). Implicit in Eq. (14) is the assumption that diffusion occurs via nearest-neighbor hops, and that transition-state recrossing does not occur. This is an excellent assumption for the systems studied here, as diffusion coefficients obtained via Eqs. (13) and (14) are fully consistent. To estimate D using Eq. (14), we obtained the average of nk_{TST} from the average of simulated residence times of an atom in a binding site.

III. RESULTS

Figure 3 shows an Arrhenius plot of dimensionless tracer-diffusion coefficients $D^\star=D/(\sigma^2\epsilon/m)^{1/2}$ obtained from four different simulations: one set of points is from *unboosted* MD simulations, two sets are obtained in accelerated MD simulations using the bias potential in Eq. (3), and one set of points is obtained in accelerated MD simulations using the bias potential given by Eq. (7). The two sets of results using the bias potential in Eq. (3) are obtained with the boosting parameters ($V_b=-3.355\epsilon$, $c=0.5$, $\gamma=0.78$), which produces a biased PES with the same shape as the original, and with ($V_b=-3.355\epsilon$, $c=0.5$, $\gamma=0.05$), which produces subwells in the PES [similar to those shown in Fig. 1(a) with $\gamma=0.1$]. The set of results using the bias potential in Eq. (7) is obtained with the boosting parameters ($V_b=-3.104\epsilon$, $c=2.18$, $n=1.0$), which produces a biased PES with the same shape as the original. It should be noted that the maximum energy of a single particle (the adatom) at the transition state in this system is -2.854ϵ, and the maximum energy of a single particle (the adatom) at the minimum is -4.356ϵ. To obtain the various diffusion coefficients shown in Fig. 3, averages are computed over 5–15 runs ranging in length from 5–10 million time steps. Generally, the largest number of runs and the longest runs are needed to obtain good statistics for the lowest temperatures probed in each set of results. From Fig. 3, we see that the different, tracer-diffusion coefficients agree well with one another, and all exhibit Arrhenius behavior. In addition, the slope of a line fit through all the points yields an activation barrier of $E_d=(1.48\pm0.02)\epsilon$, which is in good agreement with the static value of $E_d=1.50\epsilon$. For all simulations, the adatom conducts hops between neighboring binding sites. We confirmed that the distribution of residence times of adatoms in binding sites is consistent with a Poisson process. Similar to our findings in a previous study,[13] the introduction of subwells into the modified PES does not lead to any appreciable deviations of the diffusion coefficients attainable in accelerated MD simulations from the correct results obtained in an unbiased MD simulation.

Of central interest is the extent to which the local boost method can accelerate MD simulations. This can be characterized by the boost b, where

$$b=\frac{1}{n\Delta t}\sum_{i=1}^{n}\Delta t_i', \tag{15}$$

where $\Delta t_i'$ for time step i is given by Eq. (12), Δt is the MD time step, and n is the number of MD steps. The boost indicates the times that can be reached in boosted MD simulations relative to times in *unboosted* MD simulations. Note that in an *unboosted* MD simulation, the boost is unity. In Fig. 4, we show the average boosts as a function of dimensionless temperature ($T^\star=k_BT/\epsilon$) obtained from the three boosted simulations shown in Fig. 3. For all three data sets, the boost increases as the temperature decreases. At $T^\star=0.21$, the highest temperature probed, b ranges from 3 to 7, while for $T^\star=0.0625$, the lowest temperature probed to exhibit sufficient adatom mobility to compute a diffusion coefficient, boosts on the order of 10^5 can be achieved. In effect, boosts of such magnitude extend the time scale of accelerated MD simulations into the ms regime.

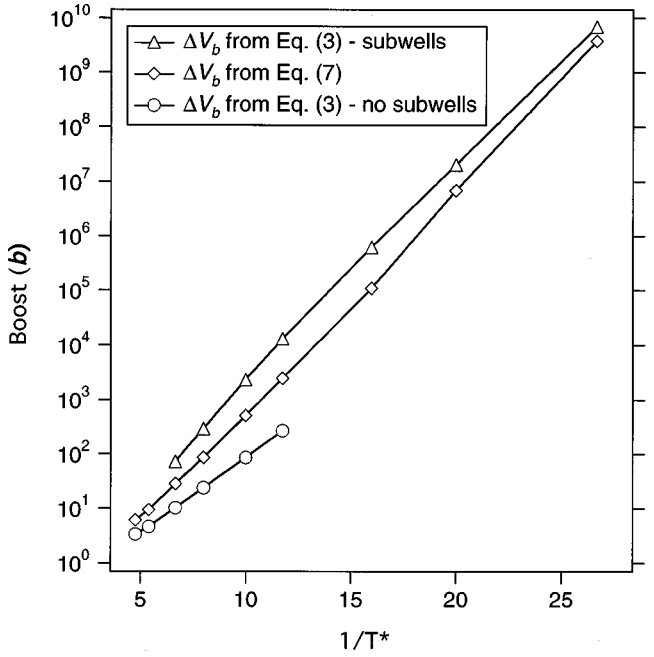

FIG. 4. Arrhenius plot of the boost b obtained from Eq. (15) as a function of dimensionless reciprocal temperature $T^\star$ (as defined in the text) for biased MD simulations using Eq. (3) (triangles, circles) and Eq. (7) (diamonds). The lines are intended to guide the eye.

From Eqs. (11) and (12), it can be seen that the boosted time step increases exponentially with increasing β, thereby making large boosts possible at low temperatures. Also, in systems with larger depths of the potential wells, the values of ΔV_b can be larger, which, in turn, will result in greater boosts [cf., Eq. (11)]. We also see from Eq. (11) that the slopes in Fig. 4 reflect the average bias potential ΔV_b given to the adatom by the different boosting functions. In all cases studied here, the average ΔV_b is less than ϵ and smaller than the diffusion barrier. Thus, as the temperature drops, adatom mobility declines more rapidly than the boost increases. Indeed, we observed almost no adatom mobility in our simulations at temperatures lower than $T^\star = 0.0625$, even with boosts of around 10^{10} at $T^\star = 0.0375$. The largest boosts can be obtained using the bias potential in Eq. (3) for a PES with subwells. In this case, the PES becomes convex near the minimum [cf., Fig. 1(a), $\gamma = 0.1$], and ΔV_b is large compared to the cases for which the biased PES retains the shape of the original one. The large boosts obtained at low temperatures are highly conducive to long-time simulations.

In the examples presented above, we introduced the local boost method, and demonstrated its accuracy for simple, model systems. However, we believe that the most significant applications for accelerated MD simulations will be for complex systems containing many different types of minima and transition states. Thus it is desirable to extend the method to more complex systems. For this purpose, we introduce multiple boosting thresholds into the method. The need for multiple boosting-threshold energies is demonstrated in Fig. 5, where we depict two uniform one-dimensional sections of a multidimensional PES (a) and a one-dimensional, heterogeneous PES (b). In the PES depicted in (a), the system evolves via two parallel rate processes, and in (b) various minima are encountered in a serial manner. It is likely that dynamical evolution in complex systems occurs via some combination of parallel and serial rate processes. Considering accelerated MD simulations of dynamics on these surfaces, it is clear that with a *single* boosting-threshold energy, the local boost method will not be effective. In (a) the dynamics will not be boosted at all because there will always be a particle with an energy above the lowest transition-state energy, and in (b) the dynamics will only be boosted when the system is near the lowest-energy minimum. By introducing multiple boosting-threshold energies corresponding to various minima, the effectiveness of the Local Boost method can be improved. We demonstrate this in a simple example.

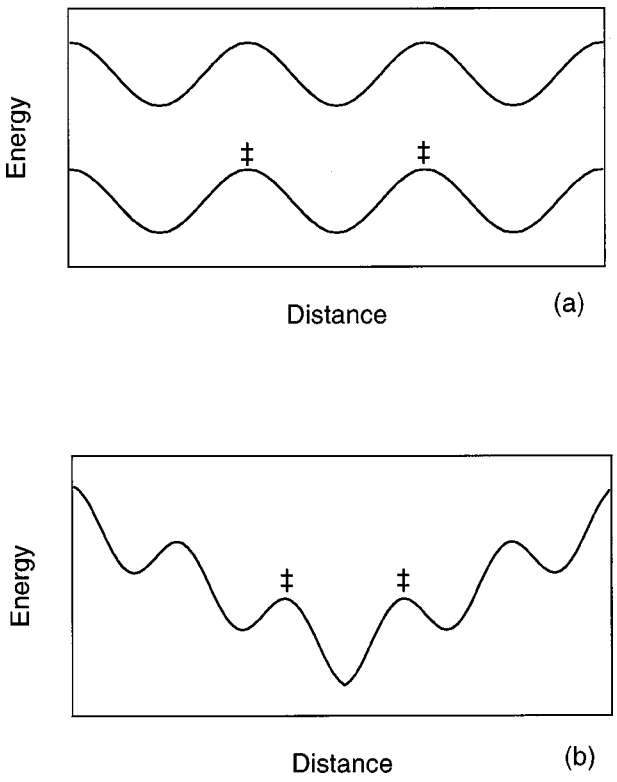

FIG. 5. Schematic depicting the PES in two possible scenarios when multiple rate processes occur. In (a), we show two one-dimensional sections of the PES for two rate processes occurring in parallel, and in (b) we show a one-dimensional PES on which various, different rate processes can occur in series. In both (a) and (b), the lowest-energy transition states are indicated by ‡.

We consider two different versions of the scenario presented in Fig. 5 for our example. In the first, we consider two particles diffusing in parallel: one on the Lennard-Jones fcc(111) surface described above, and one on a modified Lennard-Jones fcc(001) surface. We add a constant to the potential energy for the Lennard-Jones fcc(001) surface, such that the single-particle minimum and transition-state energies are 0.644ϵ and 2.146ϵ, respectively. Note that the diffusion-energy barrier on the modified fcc(001) surface is the same as in our example above (cf. Fig. 3). For the fcc(111) surface, the single-particle minimum and transition-state energies are -3.522ϵ and -4.122ϵ, respectively, while the TST

diffusion barrier is 0.6ϵ. Our second example also involves particles diffusing in parallel—this time both particles diffuse on fcc(001) surfaces—one on the Lennard-Jones fcc(001) surface described above, and one on the modified Lennard-Jones fcc(001) surface described above. Although our examples have not been constructed to explicitly represent actual physical systems, one could anticipate this general scenario to occur for two adatoms diffusing on different facets of a polycrystalline solid surface.

In both systems described above, the dynamics would not be accelerated at all with a single boosting-threshold energy because one single-particle energy will always exceed the lowest-energy transition state. By incorporating multiple boosting-threshold energies, we have a chance to accelerate the dynamics. We use two threshold energies in each example to implement this protocol. For the fcc(001)/fcc(111) system, we use $V_{b,1}=1.896\epsilon$ [fcc(001)] and $V_{b,2}=-3.722\epsilon$ [fcc(111)]. We use $V_{b,1}=-3.104\epsilon$ and $V_{b,2}=1.896\epsilon$ for the fcc(001)/fcc(001) system. For all systems, we employ the same boosting parameters as those in the simulations of single-atom diffusion (cf. Fig. 3). Parallel MD simulations of particle diffusion on the two surfaces are run for each system. At each time step, we determine ΔV_{min}, considering the boosting thresholds for both minima, as described below Eq. (7). We find for the fcc(001)/fcc(111) system that, for all temperatures at which an appreciable boost can be achieved, the boost is almost always based on the (relatively) shallow minimum associated with the fcc(111) surface. For the temperatures probed, this boost is significantly less than the boosts we observe for diffusion of a single atom on the fcc(001) surface (cf. Fig. 4). Over the time scales that can be probed in these simulations, we observe appreciable motion of the particle on the fcc(111) surface. However, as would be expected for the time scales that we can probe at low temperatures in these simulations with several million time steps, the particle on the fcc(001) surface remains almost totally localized in a single minimum. We believe that our observation here is a general feature inherent in accelerated MD simulation methods, such as the local boost method and the method by Voter[8]: *when such methods are properly applied to rate processes occurring in parallel, the ''fast'' process (with the largest TST rate constant) will determine the magnitude of the boost.*

Our second example of the fcc(001)/fcc(001) system is more interesting. Since the TST rate constants are the same for diffusion on both surfaces, the boost alternates randomly between the two particles. Although the biased PES in this study is very similar to that used for the study of single-atom diffusion on the fcc(001) surface, the overall boost, shown for different temperatures in Fig. 6, is about half that in the single-particle simulations. This illustrates a second feature of the local boost method applied to parallel rate processes. To understand this feature, we recognize that the overall boost given by Eq. (15) can be expressed as

$$b=(1-P_{boost})+P_{boost}b_{boost}, \tag{16}$$

where P_{boost} is the probability that the system is boosted in a given time step, and b_{boost} is the average value of the boost

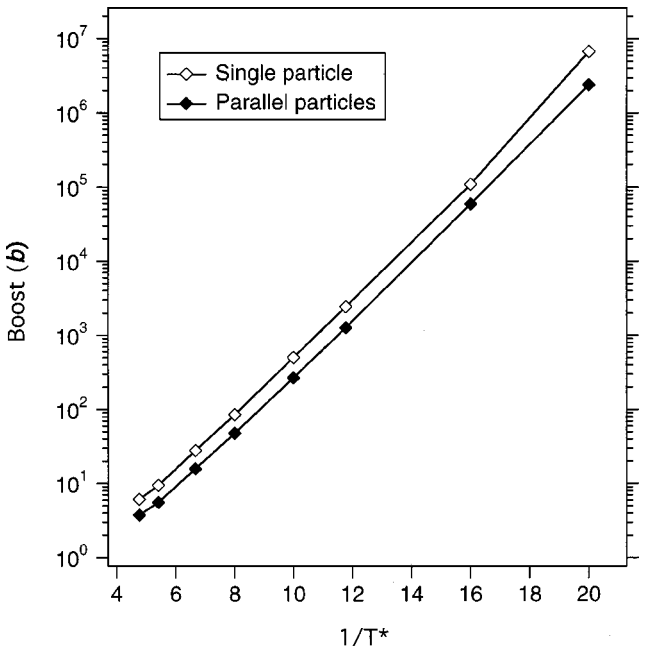

FIG. 6. Arrhenius plot of the boost b obtained from Eq. (15) as a function of dimensionless reciprocal temperature $T^\star$ (as defined in the text) for biased MD simulations using Eq. (7) for a single particle (open diamonds) and for two particles diffusing in parallel in the fcc(001)/fcc(001) system described in the text (filled diamonds). The lines are intended to guide the eye.

given that the system is boosted and $w>1$ [cf. Eq. (11)]. When we boost parallel rate processes the overall boost b declines for two reasons. First, there is a higher probability that the potential energy of any single atom will exceed the boosting threshold in a given time step, and P_{boost} declines. Second, when the system is boosted, the boost (b_{boost}) is less because the highest atom potential energy is more likely to fall close to a boosting threshold. To characterize the contributions of these factors to the decline of the boost for the parallel particles, we obtained P_{boost} and b_{boost} from both the single-particle and parallel-particle simulations using Eq. (7) for the boost. P_{boost} is given by $P_{boost}=m/n$, where m is the number of times the system is boosted out of n MD steps. Knowing P_{boost} and the overall boost b, we obtain b_{boost} from Eq. (16). We find that P_{boost} for parallel particles is much the same as that for the single particle—deviations are less than 6% over the temperatures probed. Differences between b_{boost} for a single particle and for two parallel particles are more significant, and it is evident that the decrease in this quantity governs the decline in the overall boost for the fcc(001)/fcc(001) system. Note that when the number of parallel particles increases, both P_{boost} and b_{boost} are expected to approach zero.

In Fig. 7, we show an Arrhenius plot of the diffusion coefficients for the fcc(001)/fcc(001) parallel particles. For comparison, we also include the diffusion coefficients of a single particle, boosted via Eq. (7) and shown in Fig. 3. We see that the diffusion coefficients coincide very well with one another, which indicates the accuracy of the local boost method when multiple boosting thresholds are used. Although here we apply the local boost method to simple

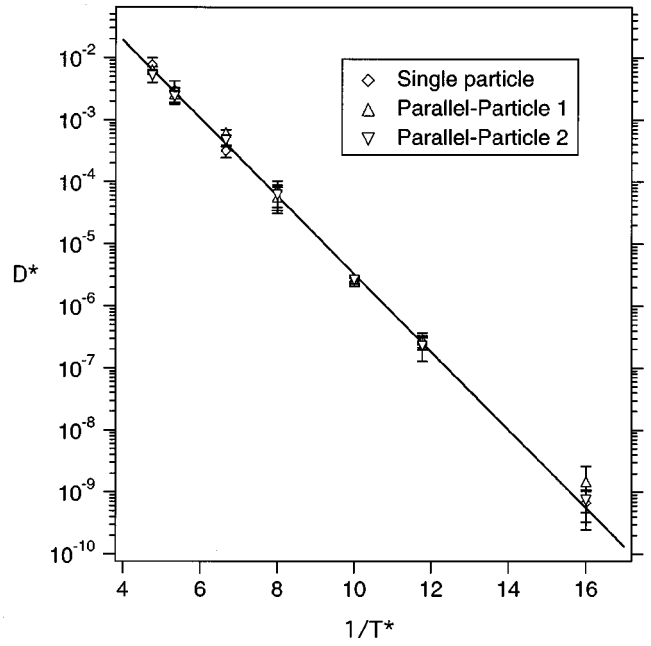

FIG. 7. Arrhenius plot of dimensionless tracer-diffusion coefficients $D^{\star}$ (as defined in the text) obtained via Eqs. (13) and (14) vs dimensionless reciprocal temperature $T^{\star}$ (as defined in the text). Results are shown for biased MD simulations using Eq. (7) for a single particle (diamonds) and for each of the two particles diffusing in parallel in the fcc(001)/fcc(001) system described in the text (triangles, inverted triangles). The solid line is a fit through all data points obtained for the single-particle case.

examples in which transition-state energies are known, the method could be extended to more complex systems, in which transition-state energies are not known *a priori*. This is because the single-particle energy is a function of a limited number of neighbors within the potential cutoff distance. For many systems, the number of ways that atoms are arranged locally around a single atom is limited, and so is the number of energy minima. Boosting-threshold energies can be selected based on the energies of particles in minima and/or can be dynamically adjusted during a trial run. This procedure should allow for accurate and efficient simulation of many different types of rate processses in materials.

IV. SUMMARY AND CONCLUSIONS

In summary, we presented the local boost method to accelerate MD simulations of rare events. In this method, a bias potential is used to raise the potential energy near potential-energy minima, so that the dynamics are accelerated. The bias potential is turned on (off) when the potential-energies of all atoms are below (above) preset, boosting-threshold values. This feature allows the method to be implemented with minor modification to a conventional MD code and minimal computational overhead. Using principles of importance sampling, we related temporal evolution on the biased PES to that on the original one, and demonstrated that this can be correctly done in some examples of adatom diffusion on Lennard-Jones fcc surfaces. In these studies, boosts of over 10^5 could be achieved, and we discussed how the boost for a particular system depends on the depth of the potential-energy minima as well as the temperature. We demonstrated how the method can be implemented with multiple-boosting thresholds in simple examples of the parallel diffusion of adatoms on Lennard-Jones fcc surfaces. Here we found and discussed that the ''fast'' atom with the largest TST rate constant should determine the overall boost. Our results show that the local boost method with multiple boosting thresholds holds significant promise for application in large-scale MD simulations.

ACKNOWLEDGMENTS

This research was supported by NSF Grant No. DMR-9617122.

[1] R. Marcelin, Ann. Phys. (N.Y.) **3**, 120 (1915).
[2] E. Wigner, Z. Phys. Chem. Abt. B **19**, 203 (1932).
[3] H. Eyring, J. Chem. Phys. **3**, 107 (1935).
[4] H.C. Kang, and W.H. Weinberg, J. Chem. Phys. **90**, 2824 (1989).
[5] K.A. Fichthorn and W.H. Weinberg, J. Chem. Phys. **95**, 1090 (1991).
[6] H. Metiu, Y.-T. Lu, and Z. Zhang, Science **255**, 1088 (1992).
[7] A.F. Voter, Phys. Rev. B **34**, 6819 (1986).
[8] A.F. Voter, J. Chem. Phys. **106**, 4665 (1997).
[9] A.F. Voter, Phys. Rev. Lett. **78**, 3908 (1997).
[10] A.F. Voter, Phys. Rev. B **57**, R13985 (1998).
[11] H. Grubmüller, Phys. Rev. E **52**, 2893 (1995).
[12] M.M. Steiner, P.-A. Genilloud, and J.W. Wilkins, Phys. Rev. B **57**, 10 236 (1998).
[13] S. Pal and K.A. Fichthorn, Chem. Eng. J. **74**, 77 (1999).
[14] N. Metropolis, A. Rosenbluth, M. Rosenbluth, M. Teller, and E. Teller, J. Chem. Phys. **21**, 1087 (1953).
[15] G.M. Torrie, and J.P. Valleau, J. Comput. Phys. **23**, 187 (1977).
[16] E.K. Grimmelmann, J.C. Tully, and E. Helfand, J. Chem. Phys. **74**, 5300 (1981).
[17] Note that the formalism is useful as long as $V_{max}(\{\mathbf{R}\})<0$. Since, for many problems in condensed-phase systems, $V<0$ is generally satisfied (or can be imposed), the method can be used satisfactorily.
[18] M.S. Daw and M.I. Baskes, Phys. Rev. Lett. **50**, 1285 (1983).
[19] F.H. Stillinger and T.A. Weber, Phys. Rev. B **31**, 5262 (1985).
[20] D.E. Sanders, and A.E. DePristo, Surf. Sci. Lett. **264**, L169 (1992).
[21] J.M. Cohen and A.F. Voter, Surf. Sci. **313**, 439 (1994).
[22] C. Kittel, *Introduction to Solid-State Physics*, 6th Ed. (Wiley, Singapore, 1991).
[23] M. P. Allen and D. J. Tildesley, *Computer Simulations of Liquids* (Clarendon, Oxford 1989).
[24] D.J. Evans, J. Chem. Phys. **78**, 3297 (1983).
[25] D. Brown and J.H.R. Clarke, Mol. Phys. **51**, 1243 (1984).